

34 nervous system, digestive system, reproductive system, and urinary system by
35 affecting major organs.² Conventionally, sodium carbonate is used to desulfurize
36 and neutralize the effluent, separating the lead in the form of sludge.³ According
37 to a 2011 market survey report by the Mineral Economics Division, Indian Bureau
38 of Mines, there were only 316 registered recyclers in India in 2010, including five
39 in the Chhattisgarh state. However, many backyard smelters dispose of effluent
40 without any treatment to increase profits. These smelters require an efficient and
41 inexpensive technique to treat the effluent and keep the Pb(II) concentration in the
42 discharge within safe limits (0.1 mg L^{-1}).

43 Various methods are available to remove Pb(II) from water, such as precipit-
44 ation, membrane separation, ion exchange, electrocoagulation, filtration and ads-
45 orption.⁴ Adsorption is a widely used technique due to its operational simplicity,
46 cost-effectiveness and low capital cost. Activated carbon is often used in water
47 treatment processes due to its different chemical characteristics, porous structure,
48 and high surface area.⁵ Activated carbon is available in both powder (PAC) and
49 granular (GAC) forms, with PAC having larger pores and GAC having smaller
50 internal pores and a lower adsorption rate than PAC. GAC is preferred over PAC
51 due to its ease of handling and disposal and reduced losses during operation.⁶
52 Several investigations have utilized GAC to treat wastewater, including removing
53 lead from aqueous solutions by Dwivedi *et al.*, removing copper, zinc and lead
54 ions by Chen and Wang, removing amoxicillin from water by Franco *et al.*, rem-
55 oving phenol from synthetic water by Sulaymon *et al.* and removing cadmium and
56 lead by Jusoh *et al.*⁶⁻¹⁰

57 Activated carbon is a widely used adsorbent for water treatment because of its
58 porous structure, abundant active sites, functional groups, and high surface area.
59 However, its adsorption capacity is limited, and researchers have modified it using
60 chemical agents to enhance its efficiency by promoting chemisorption of pollutants
61 on the surface. Wang *et al.* modified GAC with magnesium, resulting in an
62 increased adsorption capacity from 3.47 to 8.08 mg g^{-1} for the adsorption of
63 Cd(II).¹¹ Fan and Anderson used the manganese oxide for the removal of Cu(II)
64 and Cd(II), and Yao *et al.* modified activated carbon derived from rice husk using
65 nitric acid, which increased its uptake capacity by improving the surface charac-
66 teristics and porous structure.^{12,13} In another study, Jiang *et al.* found that modify-
67 ing activated carbon with HNO_3 as an impregnating agent after oxidizing it using
68 concentrated sulfuric acid increased the mesoporous volume, specific surface area,
69 and uptake capacity for the separation of dibenzothiophene and methylene blue.¹⁴

70 The modification of activated carbon with nitric acid has been widely; how-
71 ever, this study investigates the effect of modification on granular activated carbon.
72 HNO_3 -modified GAC was used for the first as an adsorbent for the treatment of
73 LAB recycling unit effluent. The characteristics of GAC and HNGAC were ana-
74 lyzed using SEM, FTIR and XRD to determine the effect of modification. The

75 adsorption experiments were conducted based on a Taguchi orthogonal L16 array
 76 (4^3) with four levels of the parameters: adsorbent dose, retention time and pH.
 77 The parameters were optimized using the signal-to-noise ratio (*SNR*) obtained
 78 from Taguchi analysis.

79 EXPERIMENTAL

80 *Wastewater*

81 The wastewater of a lead-acid battery (LAB) recycling plant was obtained from a smelter
 82 in Raipur, Chhattisgarh, India. The pH of the effluent was 1.2, and the concentration of Pb(II)
 83 was 11.2 mg L^{-1} . Prior to the batch adsorption study, the pH of the wastewater was adjusted
 84 using standard solutions of sodium hydroxide and hydrochloric acid.

85 *Adsorbent*

86 Granular activated carbon (GAC) was commercially procured and improved using nitric
 87 acid following the process described by El-Wakil *et al.*¹⁵ To prepare the modified GAC, a
 88 mixture of HNO_3 and distilled water in a 1:1 ratio was heated to $110 \text{ }^\circ\text{C}$. Then, 1 g of GAC was
 89 added to 5 mL of the heated solution and heated for 3 h. The resulting solution was filtered, and
 90 the solid fraction was collected and washed with distilled water until the pH reached 6. Finally,
 91 the nitric-acid-modified GAC (HNGAC) was dried for 24 h at $100 \text{ }^\circ\text{C}$ in a hot air oven.

92 *Characterization*

93 The surface functional groups of the adsorbents were analyzed using FTIR (Bruker, Alpha
 94 Model) within the $4000\text{--}400 \text{ cm}^{-1}$ range. The Zeiss EVO Series scanning electron microscope
 95 (SEM) was used to obtain surface micrographs and elemental composition of the adsorbents
 96 before and after the nitric acid modification. A PANalytical multifunctional XRD analyzer was
 97 used to obtain XRD spectra to determine the surface nature of the adsorbents. Standard ASTM
 98 methods were followed for proximate analysis.

99 *Batch adsorption and optimization*

100 A three factor, four level Taguchi L16 orthogonal array was obtained using Minitab 18.0
 101 to perform the experiments. The three factors were initial pH of the wastewater (1.5, 3, 4.5, 6),
 102 dose ($0.1, 0.4, 0.7, 1.0 \text{ g (50 mL)}^{-1}$) and contact time (30, 60, 90, 240 min, Table I). For batch
 103 adsorption, a fixed amount of HNGAC was added to 250 ml of wastewater in an Erlenmeyer
 104 flask and kept in an orbital shaker for a defined time at $30 \text{ }^\circ\text{C}$ and 100 rpm. The Pb(II) con-
 105 centration of the filtered effluent was analyzed using an atomic absorbance spectroscope (ECIL,
 106 India). Experimental runs were performed in duplicate and average values were reported. Eqs.
 107 (1) and (2) were used to determine the removal of Pb(II) and the uptake capacity of the ads-
 108 orbent, respectively:

$$109 \quad \text{Removal of Pb(II)} = 100 \frac{c_0 - c_e}{c_0} \quad (1)$$

$$110 \quad q_e = \frac{c_0 - c_e}{m} V \quad (2)$$

111 where c_0 and c_e are the initial and final concentration of Pb(II) in the effluent, respectively. V is
 112 the volume of effluent and m is the mass of adsorbent.

113 Taguchi analysis, which uses a signal-to-noise ratio (*SNR*), was used to optimize the param-
 114 eters and determine the optimal levels and their contribution to achieving the desired res-
 115 ponse.¹⁶ *SNR* analysis utilizes three response characteristic functions based on the minimization,

116 maximization and nominalization of the responses.¹⁷ In this study, a larger-the-better character-
 117 istic function was used for *SNR* analysis since the goal was to recover Pb(II), as represented:

$$118 \left(\frac{S}{N}\right)_{\text{Larger is better}} = -10 \log\left(\frac{1}{n} \sum_{i=1}^n \frac{1}{y_i^2}\right) \quad (3)$$

119 where y_i is the response and n is the number of experiments performed. The response factors
 120 were optimized using Minitab version 18.1. The significance and effect levels of the various
 121 factors in the batch adsorption study were determined using ANOVA analysis.

122 TABLE I. Batch adsorption parameters and their levels

Factor	Name	Level 1	Level 2	Level 3	Level 4
P	pH	1.5	3.0	4.5	6.0
D	Dose, g (50 mL) ⁻¹	0.1	0.4	0.7	1.0
T	Time, min	30	60	90	240

123

RESULTS AND DISCUSSION

124 *Characterization*

125 Fig. 1 shows a comparison of the FTIR spectra of GAC and HNGAC. After
 126 modification, the intensity of the surface functional group O–H, which corresponds
 127 to the peak at 3441 cm⁻¹ in GAC, increased and is represented by the peak at 3448
 128 cm⁻¹ in HNGAC. The signal at 2926 cm⁻¹ in GAC indicates the presence of weakly
 129 bonded methyl and methylene groups (vibrational C–H bond). These C–H groups
 130 were oxidized and vanished from the HNGAC spectra following modification. It is
 131 evident that following modification, the peak at about 1630 cm⁻¹ in GAC, which is
 132 attributed to C=O groups, became noticeably more intense in HNGAC. The small
 133 peak in both spectra at around 1400 cm⁻¹ could be due to the presence of –CH₂ and
 134 –CH₃ groups. The peaks in the 1000–1200 cm⁻¹ region can be attributed to C–O
 135 stretching and O–H bending vibrations of ether, lactonic and phenol. The peak in the
 136 HNGAC spectrum at 607.50 cm⁻¹ may be due to newly formed surface groups of
 137 oxygen and nitrogen-containing groups.^{18–21}

138 In Fig. 2, SEM micrographs of GAC and HNGAC are presented. GAC has an
 139 irregular porous structure and a rough surface. Acid treatment with nitric acid de-
 140 creased the internal micropores of GAC and removed impurities from its surface.
 141 Because nitric acid is a potent oxidant, the acid treatment created canal-like meso-
 142 pores on the surface, which reduced the pore volume and surface area.^{22,23} The
 143 impregnation of nitric acid reduced the microporous pore volume and specific sur-
 144 face area of the activated carbon, as found by Jiang *et al.*²⁴ EDS elemental analysis
 145 showed that impurities from GAC were removed and oxygen-containing groups
 146 increased after acid treatment. Moreover, HNGAC was found to contain nitrogen,
 147 indicating that nitrogen-containing groups were formed on the surface after modi-
 148 fication.

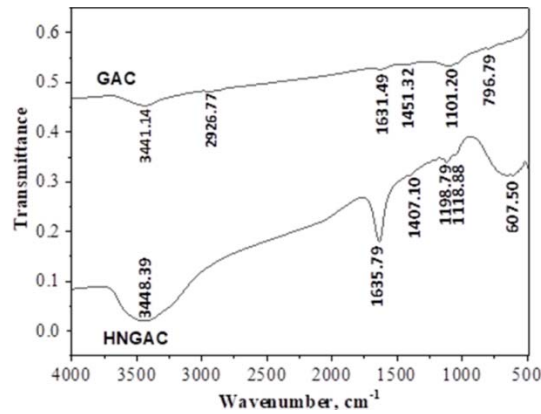


Fig. 1. FTIR spectra of GAC and HNGAC in the wavenumber range of 500–4000 cm^{-1} .

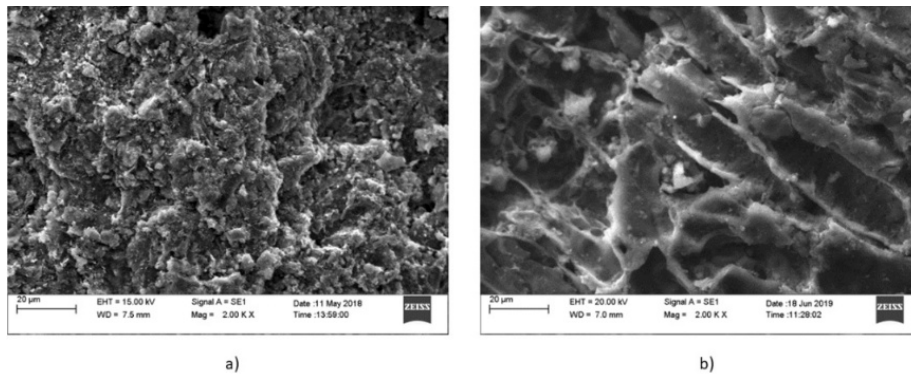


Fig. 2. Surface morphology images of: a) GAC and b) HNGAC obtained by SEM.

The crystalline or amorphous character of GAC and HNGAC was determined using the XRD spectra shown in Fig. 3. The peaks at 2θ 26 and 42° correspond to the (002) and (100) diffraction planes, respectively, and signify the amorphous

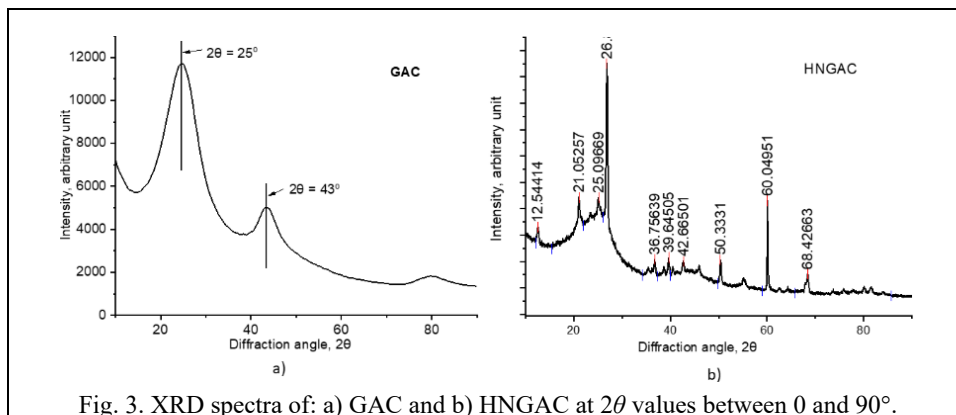


Fig. 3. XRD spectra of: a) GAC and b) HNGAC at 2θ values between 0 and 90° .

149
150

151
152

153
154
155

156 nature of activated carbon. The diffraction pattern of HNGAC exhibited several
 157 diffraction peaks, showing an increase in crystallinity due to modification. Similar
 158 effects of HNO₃ modification on adsorbent prepared from olive tree prune waste
 159 were observed by Calero *et al.*²⁵

160 *Taguchi optimization*

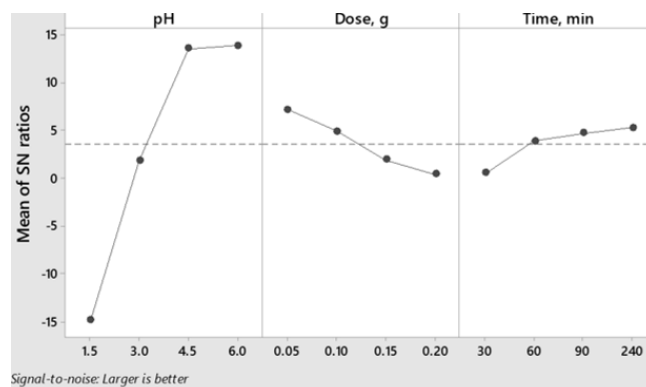
161 Three parameters at four different levels were used in the batch adsorption study
 162 using the Taguchi L16 orthogonal array. Table II displays the results for each run's
 163 adsorbent capacity and Fig. 4 displays the mean signal-to-noise ratio (*SNR*) plot for
 164 every variable associated with HNGAC's uptake capacity. It was found that while
 165 the *SNR* value decreased with increasing dose, it increased with increasing pH and
 166 time. At P4-D1-T4, the mean *SNR* value was highest. The optimal factor values were
 167 found to be pH 6, an adsorbent dose of 0.05 g, and a contact time of 240 min, based
 168 on the maximization feature of *SNR*. Nonetheless, there was little difference in
 169 uptake capacity for pH values of 4.5 and 6, so a pH value of 4.5 could be selected
 170 from an economic perspective for both adsorbents. The *SNR* analysis revealed that
 171 pH was the most influential factor in the adsorption of lead onto HNGAC.

172 TABLE II. Taguchi experimental runs for adsorption of lead onto HNGAC and the response
 173 variable (adsorbent uptake capacity)

Exp. No.	<i>P</i> (pH)	<i>D</i> (Dose, g)	<i>T</i> (Time, min)	$q_e / \text{mg g}^{-1}$
1	P1	D1	T1	0.12
2	P1	D2	T2	0.21
3	P1	D3	T3	0.20
4	P1	D4	T4	0.21
5	P2	D1	T2	2.38
6	P2	D2	T1	1.31
7	P2	D3	T4	0.95
8	P2	D4	T3	0.77
9	P3	D1	T3	9.43
10	P3	D2	T4	5.74
11	P3	D3	T1	3.18
12	P3	D4	T2	2.92
13	P4	D1	T4	9.93
14	P4	D2	T3	5.92
15	P4	D3	T2	3.96
16	P4	D4	T1	2.54

174 To determine the significance level of the factors on the adsorbent uptake
 175 capacity, an analysis of variance (ANOVA) was carried out and is presented in Table
 176 III. As observed, the coefficient of determination (R^2) was found to be 95.71, which
 177 signifies that the ANOVA model fitted well to the data. The ratio of variance
 178 between samples to variance within samples is termed the *F*-value and it indicates

179 the parameters which affect the response largely. The initial pH of the effluent was
 180 found to have the highest significance on the adsorption of lead onto HNGAC with
 181 an F -value of 28.07, whereas the least significant factor was adsorbent dose with an
 182 F -value of 0.007.



183
 184
 185

Fig. 4. Signal to noise ratio plot for the uptake capacity of HNGAC for pH, dose and time at different levels.

186

TABLE III. ANOVA analysis for adsorption of lead onto HNGAC

Source	DF	SS	MS	F -Value	P -Value
pH	3	90.629	30.210	28.07	0.001
Dose, g	3	35.563	11.854	11.01	0.007
Time, min	3	17.743	5.914	5.50	0.037
Error	6	6.457	1.076		
Total	15	150.393			
	R^2	$R^2(\text{adj})$			
	95.71 %	89.27 %			

187

Effect of each factor

188
 189
 190
 191
 192
 193
 194
 195
 196
 197
 198
 199

The effect of pH on the adsorption of Pb(II) by HNGAC is shown in Fig. 5. The pH of the effluent has a significant impact on the adsorption process, affecting the charge on the surface and the ionization of Pb(II) in the effluent. To investigate this, the pH was varied from 1.5 to 6, as Pb(II) tends to precipitate at alkaline pH values.²⁶ At low pH values, Pb(II) and H⁺ compete for adsorption onto HNGAC and consequently result in slow adsorption. Increasing the initial pH of the effluent led to an increase in the uptake capacity of HNGAC, as the competition between hydrogen and lead ions for adsorption sites decreased. Pb(II) ions were then able to bond with functional groups like -OH and -COOH present on the adsorbent surface.^{26,27} Moreover, at high pH, the negative charge on the surface increased, as protons are removed from the functional groups present on the surface, which results in enhanced electrostatic attraction for Pb(II), thereby improving adsorption.²⁸

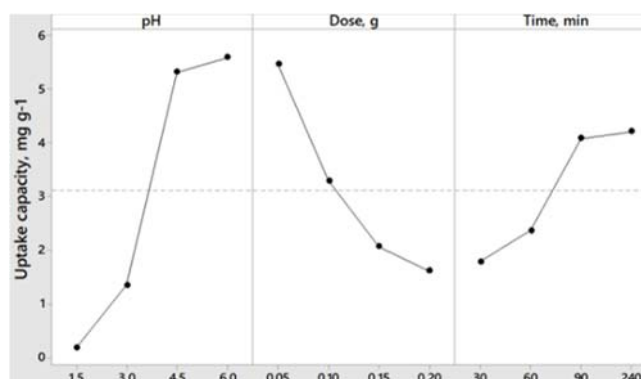


Fig. 5. Effect of initial pH, adsorbent dose and contact time on adsorption performance of HNGAC for the removal of Pb(II).

200
201
202

203 According to the results presented in Fig. 5, an increase in adsorbent dose led to
204 a decrease in the uptake capacity of Pb(II). The reason behind this trend may be the
205 existence of either unsaturated adsorption sites or overlapping and aggregation of
206 adsorption sites due to maximum adsorption being reached at a certain dose of adsorbent.²⁹

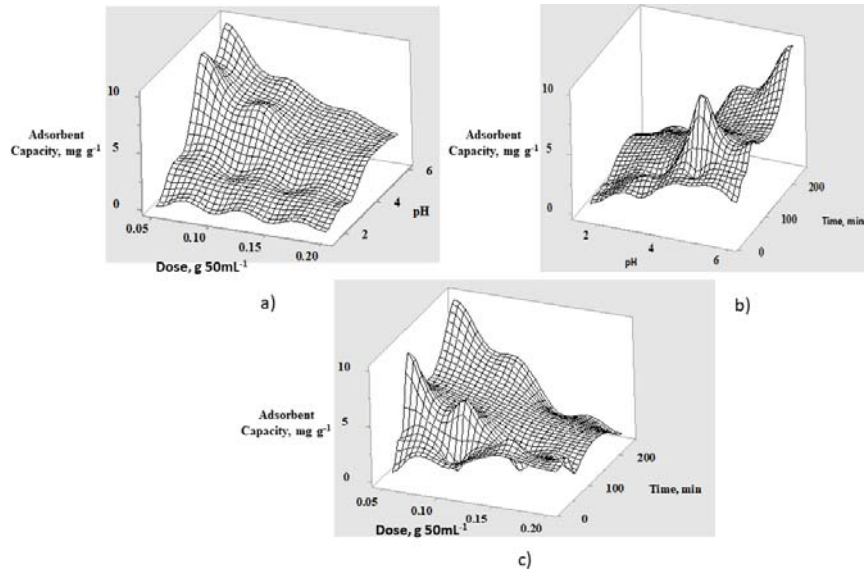
208 The effect of contact time on Pb(II) uptake capacity was investigated, and as
209 shown in Fig. 5, the uptake increased up to 90 min, after which it reached a plateau.
210 This trend could be attributed to the initial availability of more than enough active
211 sites for the adsorption of Pb(II), which became occupied over time, resulting in
212 effective utilization of the adsorbent. As the number of active sites decreased with
213 time, the competition between the lead ions in the effluent and the adsorbent surface
214 for the remaining adsorption sites slowed down the adsorption process.

215 Fig. 6 displays response surface plots that illustrate the impact of two factors
216 on the adsorption. Fig. 6a indicates that, to achieve optimal adsorbent capacity,
217 adsorbent dose should be less than 0.1 g (50 mL)⁻¹, and the pH should exceed 4.
218 This suggests that competition between Pb(II) and H⁺ decreased at higher pH and
219 that complete saturation of adsorption sites occurred at lower adsorbent doses. It
220 can be found from Fig. 6b that higher adsorbent capacity is obtained at pH > 4.5
221 and time > 80 min. This implies that insufficient interaction between the lead ions
222 and adsorbent sites prevented high absorption capacity from being reached at the
223 start of adsorption, even at high pH. High lead uptake capacity of HNGAC was
224 achieved at doses <0.1 g/(50 mL) and time > 90 min as can be observed in Fig. 6c.

225 Isotherm study

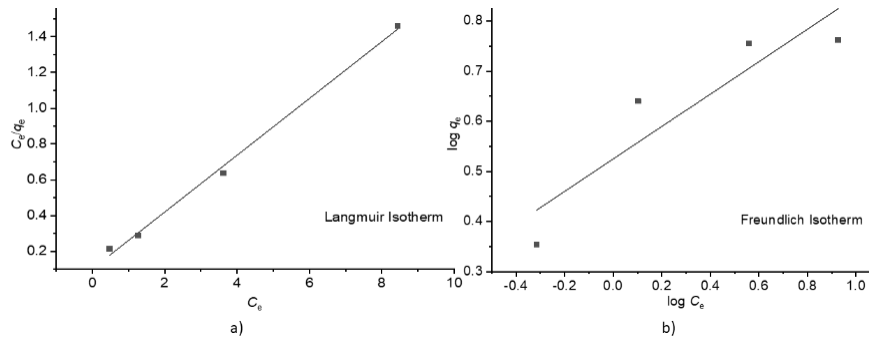
226 The fitting graphs for the Langmuir and Freundlich models fitted to the experi-
227 mental data for Pb(II) adsorption onto HNGAC are shown in Fig. 7. Table IV
228 displays the parameters of the isotherm models obtained from fitting the experi-
229 mental data. The correlation coefficient (R^2) of the Langmuir model is higher than

230 that of the Freundlich model. This shows that the adsorption equilibrium data fit the
 231 Langmuir equation and the adsorption involves monolayer adsorption. The maxi-
 232 mum monolayer adsorption capacity obtained from the Langmuir model is 9.93 mg
 233 g⁻¹ for HNGAC.



234
 235
 236

Fig. 6. Plots of simultaneous effect of two factors on lead adsorption onto HNGAC: a) initial pH and dose, b) time and pH and c) time and dose.



237
 238
 239
 240

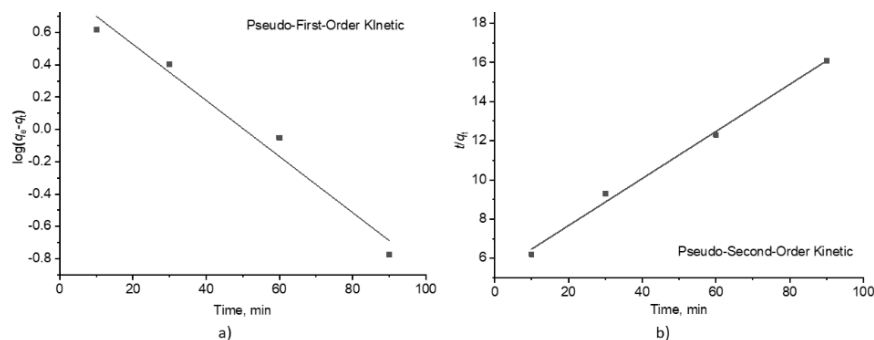
Fig. 7. Isotherm plots for Pb(II) adsorption onto HNGAC: a) Langmuir isotherm and b) Freundlich isotherm (pH 4.5; time 60 min; speed 100 rpm; volume 50 mL; temperature 30 °C; dose 2 g L⁻¹).

241 TABLE IV. Parameters of the isotherm models for Pb(II) adsorption onto HNGAC.

Langmuir			Freundlich		
$q_m / \text{mg g}^{-1}$	$K_L / \text{L mg}^{-1}$	R^2	$1/n$	$K_F / \text{mg g}^{-1} ((\text{mg L}^{-1})^{1/n})^{-1}$	R^2
9.90099	0.639240506	0.99	0.323	1.688769234	0.836

242 *Kinetic study*

243 Both pseudo-first-order and pseudo-second-order kinetic models were used to
 244 assess the adsorption of Pb(II) onto HNGAC. Fig. 8 displays the kinetic plots, while
 245 Table V provides the correlation coefficient and kinetic model parameters. Because
 246 of its higher correlation coefficient of 0.99, the pseudo-second-order kinetic model
 247 better describes the adsorption kinetics than the pseudo-first-order. This implies that
 248 chemisorption may play a dominant role in the adsorption process. Compared to the
 249 pseudo-first-order model, the value of q_e derived from the pseudo-second-order
 250 model agrees better with the experimentally determined q_e value. Abbaszadeh *et al.*
 251 observed similar outcomes for the adsorption of Pb(II) on activated carbon from
 252 papaya peel biowaste.²⁶ They found a measured uptake capacity of 38.31 mg g⁻¹
 253 and a calculated uptake capacity of 42.55 mg g⁻¹ from the pseudo-second-order
 254 kinetics.



255
 256 Fig. 8. Kinetic study graph for lead adsorption onto HNGAC: a) pseudo-first-order model and
 257 b) pseudo-second-order model (initial pH 4.5; adsorbent dose, 0.1 g (50 mL)⁻¹; Pb(II)
 258 concentration, 10.2 mg L⁻¹).

259 TABLE V. Kinetic model parameters for Pb(II) adsorption onto HNGAC for the PFO and PSO
 260 models.

PFO			PSO		
K_1 / h^{-1}	q_e	R^2	$K_2 / \text{g mg}^{-1} \text{h}^{-1}$	q_e	R^2
0.039151	2.394082	0.973	0.002738684	8.333333	0.994

261 *Mechanism of adsorption*

262 The adsorption of Pb(II) onto the adsorbents involves physical and chemical
 263 interactions with the surface functional groups. The adsorption of Pb(II) may be
 264 caused by ion exchange interactions with surface groups like hydroxyl and carboxyl.
 265 The FTIR analysis revealed that the intensity of these groups, especially -OH and -
 266 COOH, was higher in HNGAC compared to GAC, which supports the ion exchange
 267 between adsorbent and adsorbate. It was also observed that the amount of Pb(II)
 268 uptake by HNGAC was significantly higher than that of GAC, indicating that

311 β $\frac{1}{2}$ $\text{C}\ddot{\text{A}}\text{C}\ddot{\text{U}}\text{A}\text{NOUA}$ $\frac{1}{2}$ $\text{A}\ddot{\text{A}}\text{A}$ | D , OH D | $\text{I}\ddot{\text{D}}\text{A}\mu$ | E | $\text{p}\text{C}\ddot{\text{U}}\text{A}$ $\text{p}\frac{1}{2}$ C $\text{A}\frac{1}{2}$ $\text{A}\ddot{\text{A}}\text{A}$ | γ | E $\frac{1}{2}$ $\text{p}\mu\text{C}\ddot{\text{O}}$, $\text{A}\frac{1}{2}$ F - $\text{U}\ddot{\text{O}}\text{E}\text{I}$ -
 312 $\text{A}\text{C}\ddot{\text{U}}$ \gg $\ddot{\text{U}}$ $\text{C}\ddot{\text{I}}$ 28 ,/7. 1 $\text{C}\mu\text{D}\ddot{\text{O}}\text{Y}$ $\text{A}\text{p}\frac{1}{2}$ | p | $\text{A}\ddot{\text{D}}\mu$ | $\text{N}\text{p}\frac{1}{2}$ | $\text{A}\ddot{\text{n}}$ | μ | $\text{U}\frac{1}{2}$ " $\frac{1}{2}$ $\text{U}\text{A}\text{p}\text{C}$ > D $\text{A}\ddot{\text{U}}$ $\text{A}\ddot{\text{n}}\text{O}\text{C}\ddot{\text{U}}\text{D}\text{I}\text{E}\text{A}\frac{1}{2}$ $\text{O}\frac{1}{2}$ | $\text{O}\frac{1}{2}$ U -
 313 $\text{Y}\text{D}\ddot{\text{U}}\frac{1}{2}$ " $\frac{1}{2}$ $\text{Y}\text{D}\ddot{\text{S}}\text{A}$ | $\text{Y}\frac{1}{2}$ $\text{I}\text{A}\text{C}\ddot{\text{O}}\text{n}\ddot{\text{O}}$ | D . $\text{O}\mu\ddot{\text{U}}\text{D}$ > EAC D $\text{I}\frac{1}{2}$ $\text{I}\text{A}\text{C}\ddot{\text{O}}\text{n}\ddot{\text{O}}$ | $\frac{1}{2}$ $\text{n}\ddot{\text{O}}\mu$ | $\text{O}\frac{1}{2}$ AEY $\ddot{\text{U}}$ | $\text{O}\text{C}\ddot{\text{U}}\text{U}$ | $\text{C}\mu\text{D}\ddot{\text{O}}\text{Y}$ $\ddot{\text{U}}$ |
 314 p | $\text{A}\ddot{\text{D}}\mu$ | Np | Y $\text{C}\ddot{\text{I}}\text{D}\text{A}$ $\text{I}\ddot{\text{O}}\text{E}\text{C}\text{E}$ $\text{O}\ddot{\text{E}}\text{I}\frac{1}{2}$.

(- O | Y , EAC 18. $\frac{1}{2}$ $\text{I}\text{E}\text{U}\text{A}\frac{1}{2}$, $\text{O}\ddot{\text{E}}\text{U}$ | I | $\text{O}\frac{1}{2}$ AC 22. $\text{C}\mu\text{C}\ddot{\text{O}}\text{O}$, $\text{n}\ddot{\text{O}}$ | $\text{S}\ddot{\text{U}}\text{A}$ EAC 24. $\text{I}\text{E}\text{O}\text{E}\text{Y}$ $\text{O}\ddot{\text{O}}\frac{1}{2}$ 2/24)

316

REFERENCES

- 317 1. S. Meshram, R. S. Thakur, G. Jyoti, C. Thakur, A. B. Soni, *J. Indian Chem. Soc.* **99**
 318 (2022) 100469 (<https://doi.org/10.1016/j.jics.2022.100469>)
 319 2. M. Caccin, M. Giorgi, F. Giacobbo, M. D. Ros, L. Besozzi, M. Mariani, *Desalin. Water*
 320 *Treat.* **57** (2016) 4557 (<https://doi.org/10.1080/19443994.2014.992974>)
 321 3. S. Meshram, C. Thakur, A. B. Soni, *J. Serb. Chem. Soc.* **85** (2020) 953
 322 (<https://doi.org/10.2298/JSC191103015M>)
 323 4. S. Meshram, S. Dharmadhikari, R. S. Thakur, C. Thakur, A. B. Soni, *J. Hazard. Mater.*
 324 *Adv.* **10** (2023) 10297 (<https://doi.org/10.1016/j.hazadv.2023.100297>)
 325 5. C. Thakur, I. D. Mall, V. C. Srivastava, *Theor. Found. Chem. Eng.* **48** (2014) 60
 326 (<https://doi.org/10.1134/S004057951401014X>)
 327 6. C. P. Dwivedi, J. N. Sahu, C. R. Mohanty, B. R. Mohan, B. C. Meikap, *J. Hazard. Mater.*
 328 **156** (2008) 596 (<https://doi.org/10.1016/j.jhazmat.2007.12.097>)
 329 7. J. P. Chen, X. Wang, *Sep. Purif. Technol.* **19** (2000) 157 ([https://doi.org/10.1016/S1383-](https://doi.org/10.1016/S1383-5866(99)00069-6)
 330 $5866(99)00069-6$)
 331 8. M. A. E. Franco, C. B. Carvalho, M. M. Bonetto, R. P. Soares, L. A. Féris, *J. Clean.*
 332 *Prod.* **161** (2017) 947 (<https://doi.org/10.1016/j.jclepro.2017.05.197>)
 333 9. A. H. Sulaymon, D. W. Abood, A. H. Ali, *Hydrol. Curr. Res.* **2** (2011) 1000120
 334 (<http://dx.doi.org/10.4172/2157-7587.1000120>)
 335 10. A. Jusoh, L. S. Shiung, N. Ali, M. J. M. M. Noor, *Desalin.* **206** (2007) 9
 336 (<https://doi.org/10.1016/j.desal.2006.04.048>)
 337 11. K. Wang, J. Zhao, H. Li, X. Zhang, H. Shi, *J. Taiwan Inst. Chem. Eng.* **61** (2016) 287
 338 (<https://doi.org/10.1016/j.jtice.2016.01.006>)
 339 12. H. J. Fan, P. R. Anderson, *Sep. Purif. Technol.* **45** (2005) 61
 340 (<https://doi.org/10.1016/j.seppur.2005.02.009>)
 341 13. S. Yao, J. Zhang, D. Shen, R. Xiao, S. Gu, M. Zhao, J. Liang, *J. Colloid Interface Sci.*
 342 **463** (2016) 118 (<https://doi.org/10.1016/j.jcis.2015.10.047>)
 343 14. Z. Jiang, Y. Liu, X. Sun, F. Tian, F. Sun, C. Liang, W. You, C. Han, C. Li, *Langmuir* **19**
 344 (2003) 731 (<https://doi.org/10.1021/la020670d>.)
 345 15. A. M. El-Wakil, W. M. Abou El-Maaty, F. S. Awad, *J. Anal. Bioanal. Tech.* **5** (2014)
 346 1000187 (<https://doi.org/10.4172/2155-9872.1000187>)
 347 16. M. Nandhini, B. Suchithra, R. Saravanathamizhan, D. G. Prakash, *J. Electrochem. Sci.*
 348 *Eng.* **4** (2014) 227 (<https://doi.org/10.5599/jese.2014.0056>)
 349 17. S. Meshram, C. Thakur, A. B. Soni, *Pollution* **6** (2020) 879
 350 (<https://doi.org/10.22059/poll.2020.302442.808>)
 351 18. M. A. Ramos, V. G. Serrano, C. V. Calahorra, A. J. L. Peinado, *Spectrosc. Lett.* **26**
 352 (1993) 1117 (<https://doi.org/10.1080/00387019308011598>)
 353 19. V. G. Serrano, M. A. Ramos, A. J. L. Peinado, C. V. Calahorra, *Thermochim. Acta* **291**
 354 (1997) 109 ([https://doi.org/10.1016/S0040-6031\(96\)03098-5](https://doi.org/10.1016/S0040-6031(96)03098-5))

- 355 20. V. C. Srivastava, I. D. Mall, I. M. Mishra, *J. Hazard. Mater.* **134** (2006) 257
356 (<https://doi.org/10.1016/j.jhazmat.2005.11.052>)
357 21. T. S. Anirudhan, S. S. Sreekumari, *J. Environ. Sci.* **23** (2011) 1989
358 ([https://doi.org/10.1016/S1001-0742\(10\)60515-3](https://doi.org/10.1016/S1001-0742(10)60515-3))
359 22. N. A. Kolar, S. Sharifian, T. Kaghazchi, *Turkish J. Chem.* **43** (2019) 663
360 (<https://doi.org/10.3906/kim-1810-63>)
361 23. M. Dutta, S. Mishra, M. Kaushik, J. K. Basu, *Res. J. Environ. Sci.* **5** (2011) 741
362 (<https://doi.org/10.3923/rjes.2011.741.751>)
363 24. X. Jiang, X. Lan, Y. Song, X. Xing, H. M. A. Hassan, *J. Chem.* (2019) 8593742
364 (<https://doi.org/10.1155/2019/8593742>)
365 25. M. Calero, A. Pérez, G. Blázquez, A. Ronda, M. A. M. Lara, *Ecol. Eng.* **58** (2013) 344
366 (<https://doi.org/10.1016/j.ecoleng.2013.07.012>)
367 26. S. Abbaszadeh, S. R. W. Alwi, C. Webb, N. Ghasemi, I. I. Muhamad, *J. Clean. Prod.* **118**
368 (2016) 210 (<https://doi.org/10.1016/j.jclepro.2016.01.054>)
369 27. Z. Guo, J. Zhang, Y. Kang, H. Liu, *Ecotoxicol. Environ. Saf.* **145** (2017) 442
370 (<https://doi.org/10.1016/j.ecoenv.2017.07.061>)
371 28. Y. Li, Q. Du, X. Wang, P. Zhang, D. Wang, Z. Wang, Y. Xia, *J. Hazard. Mater.* **183**
372 (2010) 583 (<https://doi.org/10.1016/j.jhazmat.2010.07.063>)
373 29. S. Meshram, C. Thakur, A. B. Soni, *Indian Chem. Eng.* **63** (2020) 460
374 (<https://doi.org/10.1080/00194506.2020.1795933>).